THE JOURNAL OF PHYSICAL CHEMISTRY Letters

pubs.acs.org/JPCL Letter

Ultrafast Laser-Induced Isomerization Dynamics in Acetonitrile

Matteo McDonnell,* Aaron C. LaForge,* Juan Reino-González, Martin Disla, Nora G. Kling, Debadarshini Mishra, Razib Obaid, Margaret Sundberg, Vít Svoboda, Sergio Díaz-Tendero,* Fernando Martín,* and Nora Berrah*

Cite This: J. Phys. Chem. Lett. 2020, 11, 6724−6729 Read Online

ACCESS | Metrics & More | Article Recommendations | Supporting Information

ABSTRACT: Isomerization induced by laser ionization in acetonitrile (CH_3CN) was investigated using pump−probe spectroscopy in combination with ion−ion coincident Coulomb explosion imaging. We deduced five primary channels indicating direct C−C breakup, single and double hydrogen migration, and H and H_2 dissociation in the acetonitrile cation. Surprisingly, the hydrogen-migration channels dominate over direct fragmentation. This observation is supported by quantum chemistry calculations showing that isomerization through single and double hydrogen migration leads to very stable linear and ring isomers, with most of them more stable than the original linear structure following ionization of the parent molecule. This is unlike most molecules investigated previously using similar schemes. By varying the delay between the pump and probe pulses, we have also determined the time scales of the corresponding dynamical processes. Isomerization typically occurs in a few hundred femtoseconds, a time scale that is comparable to that found for H and H_2 dissociation and direct molecular fragmentation.

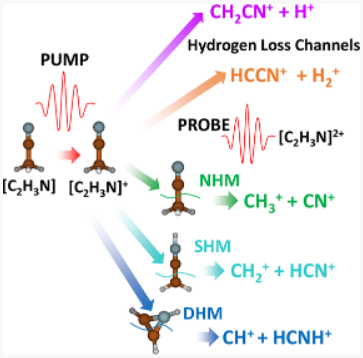

Resolving the temporal evolution of photoinduced photochemical processes is vital for understanding the underlying molecular dynamics. Isomerization induced by photoabsorption is among the most fundamental processes, since it plays a crucial role in a wide variety of biological and chemical processes.[1,2] One of the most basic mechanisms is hydrogen migration, where a hydrogen atom moves from one position in a molecule to another, resulting in a different binding structure. Due to its ubiquity, hydrogen migration has been observed in many molecular systems, from simple hydrocarbons[3] to large biomolecules.[4] Double hydrogen migration is a more exotic isomerization process, where two hydrogen atoms change sites. Recently, it was shown that single and double hydrogen migration occurs on time scales of hundreds of femtoseconds to picoseconds in ethanol.[5] For comparison, in acetylene, one of the simplest hydrocarbons, single hydrogen migration occurs within the first hundred femtoseconds.[3]

Acetonitrile (CH_3CN) is the simplest organic nitrile molecule, containing a cyano group (−C≡N) bonded to a methyl group (CH_3−). Therefore, it is an ideal system to investigate hydrogen migration because all three equivalent H atoms are located on one side of the molecule, thus avoiding any ambiguity in the identification of the origin and final destination of the migrating H atoms. In general, knowledge of light-induced dynamics in acetonitrile is intrinsically important. For example, it is a substance used as a solvent in the purification of butadiene in refineries and in the production of DNA oligonucleotides from monomers. It is also employed in battery applications due to its relatively high dielectric constant and ability to dissolve electrolytes. The electron-withdrawing character and versatile function of the cyano group makes it also highly used in organic chemistry, mainly in synthesis by bond activation of nitriles.

Coulomb explosion imaging (CEI) is a unique method to investigate molecular dynamics, where the system is multiply ionized, and upon Coulomb explosion, the kinetic energy of the constituent ionic fragments are directly measured.[6] Due to its applicability to a large variety of molecular systems, CEI is widely used, especially when combined with other techniques such as pump−probe[5,7] or coincidence[8] spectroscopy, and has recently been applied to directly visualize conical intersections[9] and probe molecular dissociation dynamics.[10] A more in-depth discussion of our specific experimental setup is given in the Methods section. Briefly, we used CEI to measure the time-resolved isomerization via femtosecond IR pump-IR probe spectroscopy. The momenta of the resulting ionic fragments from the laser−molecule interaction are measured in coincidence using the COLTRIMS technique.[11] In this pump−probe scheme, the pump laser singly ionizes the molecule while the probe pulse further excites the molecule to the dicationic state. The dynamics induced on the cation are

Received: May 1, 2020
Accepted: July 2, 2020
Published: July 2, 2020

https://dx.doi.org/10.1021/acs.jpclett.0c01344
J. Phys. Chem. Lett. 2020, 11, 6724−6729

then recorded by varying the delay between the pump and probe pulses.

Here, we show the first time-resolved measurements of isomerization in acetonitrile using IR pump-IR probe spectroscopy in combination with ion−ion coincident Coulomb explosion imaging. We observe that the isomerization channels are, in fact, some of the most dominant channels with which the acetonitrile ion fragments, resulting in much higher yields than direct breakup through the C−C bond. With the aid of quantum chemistry calculations, we interpret the enhanced isomerization channels of single and double hydrogen migration as the result of the formation of very stable linear and ring isomers after photoionization.

Figure 1 shows a portion of the two-dimensional photoion−photoion coincidence time-of-flight spectrum of acetonitrile;

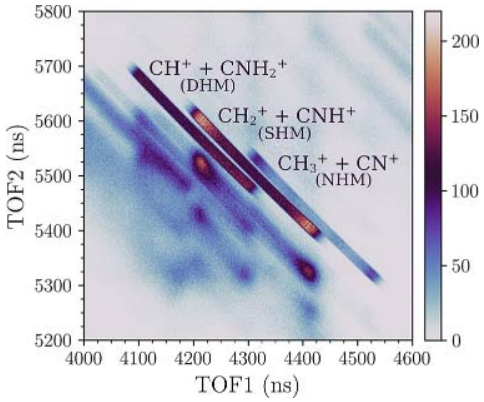

Figure 1. Two-dimensional photoion−photoion coincidence time-of-flight spectrum of CH_3CN, centered on the C−C fragmentation channels. The ion yields were obtained by integrating over all the pump−probe delays.

the full spectrum is given in the Supporting Information. The spectrum is integrated over all pump−probe delays. The observed distributions identify ions created by multiple ionization while the shape of the distribution gives information about the dissociation process.[12] The dominant two-body breakup channels observed in acetonitrile were those of H or H_2 dissociation from the parent molecule and dissociation of the carbon−carbon bond. In Figure 1, the coincidence map is centered around three sharp, negatively sloping lines associated with the latter type of fragmentation, where the labeled lines correspond to no, single, and double hydrogen migration from the methyl group to the nitrile group. $CH_3^+ + CN^+$ signifies no hydrogen migration (NHM), $CH_2^+ + CNH^+$ signifies single hydrogen migration (SHM), and $CH + CNH_2^+$ signifies double hydrogen migration (DHM). A scheme of the different steps leading to these fragments is given in the Supporting Information. These fragmentation channels result from dissociation of the molecular dication after the probe pulse, leading to back-to-back emission of the ions. Below the three sharp lines are additional, broader distributions due to higher order and/or neutral fragmentation. Additionally, the intensity of each specific dicationic channel gives information on its relative fragmentation efficiency. The relative yields of the aforementioned fragmentation channels are given in Table 1 along with those of the other two prominent fragmentation channels, H and H_2 dissociation. The relative yields are integrated over all pump−probe delays. As can be seen in

Table 1. Relative Yields, Exponential Time Constant, And Time Shift of the Fragmentation Channels of Acetonitrile[a]

channel	yield (%)	τ (fs)	t_0 (fs)
NHM	5.7	110 ± 20	240 ± 10
SHM	19.8	280 ± 30	290 ± 20
DHM	16.6	1000 ± 280	540 ± 40
H dissociation	51.9	690 ± 80	320 ± 30
H_2 dissociation	6.0	220 ± 20	230 ± 10

[a]The relative yields are integrated over all pump−probe delays.

Figure 1 and confirmed in Table 1, the H-migration channels are more prominent than the direct fragmentation of the C−C bond. Overall, this is a relatively surprising result, especially the prominence of double hydrogen migration, since it involves additional bond rearrangement.

Coincidence imaging techniques give the full momentum and kinetic energy release (KER) of the fragmentation process. Figure 2 shows the KER as a function of the probe pulse delay for NHM, SHM, and DHM. Since the pump and probe pulses have nearly identical intensities, the two pulses can be interchanged and the positive and negative delays show similar dynamics. Each fragmentation channel exhibits a broad feature centered around 5 eV, which does not show any significant shift in KER with respect to time delay. This distribution is primarily due to direct formation of the dication by a single pulse. Near time zero, the distribution does show an intensity dependence, which is especially observed in the H-migration channels. The enhanced intensity at time zero is primarily due to the temporal overlap of the two pulses; a Gaussian fit of the projection gives a $\sigma \approx 30$ fs or 70 fs fwhm.

There is a second, weaker distribution observed in all three channels which shows a strong dependence on kinetic energy as a function of pump−probe delay. This distribution appears initially at around 5 eV (associated with direct double ionization by the pump pulse as discussed above), but for increasing pump−probe delays, the distribution rapidly decreases in energy. The dynamics of this distribution, which manifests as a time-dependent decrease in KER, is due to the Coulomb repulsion of the ionic pair resulting from single ionization by the pump pulse followed by a second single ionization by the probe pulse, producing a dication. The second ionization event occurs as the molecular cation dissociates or isomerizes, so that the measured KER at a given pump−probe delay provides an instantaneous picture of the dynamics induced by the pump pulse. The two ionic fragments produced in this way repel each other following a repulsive $1/R$ potential curve, where R is the ion−ion distance.

The intensity dependence of the $1/R$ component of the three fragmentation channels is given in Figure 3 as a function of the pump−probe delay, normalized to their relative yields. Since the data showed similar intensities and time scales, the positive and negative pump−probe delays were additionally folded about time zero to increase the statistics. Each of the three fragmentation channels exhibits a similar sharp rise in intensity as the pump−probe delay increases, which saturates out at longer delays. The time scale of the rise in intensity is clearly longer for the H-migration channels than for the direct fragmentation channel. To extract time constants of the underlying process, we have fit the data with a saturating exponential function of the form:

$$1 - e^{-(\Delta t - t_0)/\tau} \quad (1)$$

https://dx.doi.org/10.1021/acs.jpclett.0c01344
J. Phys. Chem. Lett. 2020, 11, 6724−6729

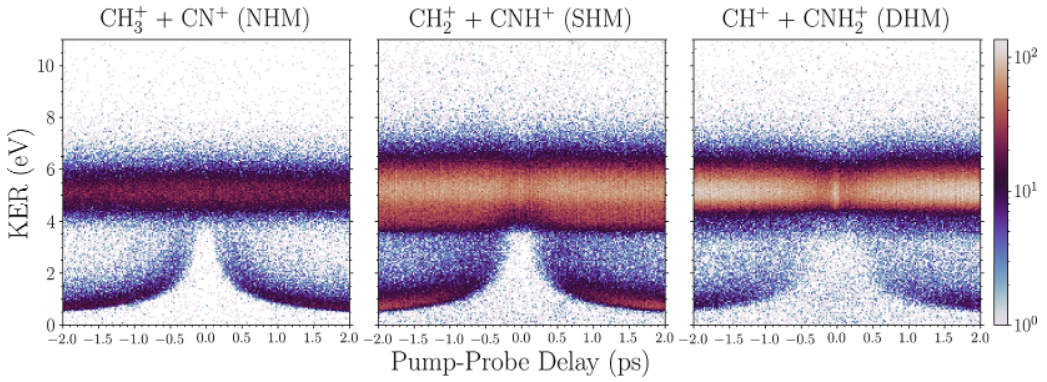

Figure 2. Kinetic energy release as a function of probe pulse delay for the three C−C fragmentation channels of acetonitrile.

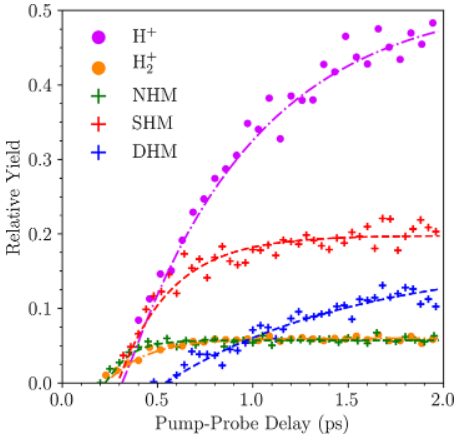

Figure 3. Intensity of the dynamic KER distribution as a function of probe pulse delay for the three C−C dissociation and two hydrogen loss channels of acetonitrile. Each channel is normalized to their relative yield and fit with the saturating exponential given in eq 1. Their best fit parameters are in Table 1. See text for details.

where Δt is the pump−probe delay, τ is the exponential time constant, and t_0 is the time shift from time zero. As will be discussed later, we attribute τ and t_0 to the molecular fragmentation time and isomerization time, respectively. The same fitting method has been applied to the KER vs pump−probe delay plots obtained for the dominant H and H_2 dissociation channels, given in the Supporting Information. The values of τ and t_0 obtained from these fits are given in Table 1. Interestingly, the dissociation time is significantly longer for the loss of atomic hydrogen compared to the loss of molecular hydrogen. It should be noted that the channels investigated here are specifically double coincidences, meaning we are fitting doubly ionized events such as $H_2^+ + CHCN^+$, rather than $H^+ + H^+ + CHCN^+$. As such, we are confident that we are tracking the fragmentation dynamics in the channel corresponding to the loss of H_2 from the singly ionized acetonitrile molecule.

Further insight into the fragmentation and isomerization processes has been obtained from quantum chemistry calculations. In a first step, we have carried out molecular dynamics simulations in the singly charged acetonitrile molecule considering several values of excitation energy, see results given in the Supporting Information. We have adopted this procedure due to the impossibility to describe the actual internal energy distribution of the cation resulting from strong field ionization of acetonitrile by using current theoretical tools. From these calculations, we have selected the molecular species associated with the dominant fragmentation channels of the singly charged acetonitrile and we have evaluated their relative energies, as well as those of the transition states leading to them, to obtain a schematic representation of the potential energy surface of the system. The latter is shown in Figure 4. The entrance channel is the vertical ionization from the neutral acetonitrile structure (∼12 eV). In addition to the canonical form of acetonitrile, we have found five stable cationic conformers: two linear structures (labeled L1 and L2 in the figure) and three cyclic structures (C1, C2, and C3). Surprisingly, four of these isomers are more stable than the canonical form of CH_3CN^+. Isomer L1, the most stable one, can easily be reached through a small energy barrier (∼0.5 eV above the entrance channel). The rest of the conformers are also energetically accessible through barriers never higher than 2.5 eV above the entrance channel. The low isomerization barriers in the potential energy surface and the high stability of these structures explain why isomerization is the dominant process after ionization with the pump pulse.

The two-fragment dissociation channels associated with NHM, SHM, and DHM processes are also shown in Figure 4 and can be considered as the exit channels. Charge location in one or the other fragment leads to quite different dissociation energies. Exit channels are reached in barrierless processes: elongation of the bonds leads to the separation of the fragments without barriers. The nature of the bonds, both in canonical CH_3CN^+ and the isomers shown, makes these structures extremely efficient energy reservoirs: strong double and triple bonds are able to absorb a vast amount of excitation energy in molecular vibrations. Thus, after ionization with the pump pulse, acetonitrile rapidly evolves toward any of the stable structures in the potential energy surface, where the excess of excitation energy is absorbed into nuclear degrees of freedom.

The time shift values, t_0, obtained in the fit and shown in Table 1 are likely due to the isomerization processes shown in Figure 4. If we consider a scenario where the ionization induced by the pump pulse brings the system into the entrance channel (vertical ionization potential in the figure), the excited singly charged canonical form (CH_3CN^+) hosts the excitation energy into nuclear degrees of freedom, and then can undergo fragmentation after a short period ($t_0 \sim 240$ fs for NHM). However, with high probability, the molecule can undergo isomerization and get trapped into the potential well of L1, where it stays for a longer time after it breaks ($t_0 \sim 290$ fs for SHM channels). Finally, further isomerization into more

https://dx.doi.org/10.1021/acs.jpclett.0c01344
J. Phys. Chem. Lett. 2020, 11, 6724−6729

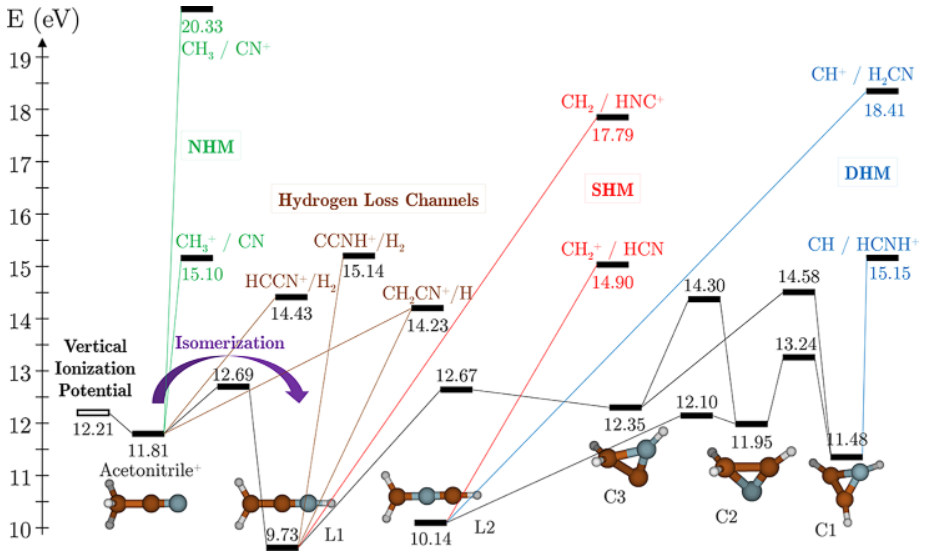

Figure 4. Critical points in the potential energy surface of singly charged acetonitrile computed at the B3LYP/6-31++G(d,p) level of theory. The open box corresponds to vertical ionization potential from the optimized neutral molecule. Optimized geometry of minima are shown together with the energy levels of the transition states that connect them. Relative energy values are referred to the neutral molecule and zero-point-energy corrected. The minima in the potential energy surface are acetonitrile$^+$, linear structures L1, L2, and cyclic structures C1, C2, and C3. NHM, SHM, and DHM stand for no-hydrogen migration, single-hydrogen migration and double-hydrogen migration, respectively.

complex structures, such as C1 or L2, reflects longer times before molecular cleavage ($t_0 \sim 540$ fs for DHM). Thus, sequential isomerization processes in subsequent potential wells provide longer time shifts.

This interpretation is further confirmed by a more in-depth analysis of the calculated potential energy surface and the measured yields for the hydrogen-loss channels. Indeed, according to Figure 4, H and H_2 dissociation (loss) are possible either directly from CH_3CN^+ or through the intermediate isomer L1. Since removing H from L1 requires less energy than removing it from CH_3CN^+ and, according to the discussion above, isomerization from CH_3CN^+ to L1 is a very efficient process, we should expect that H loss will be mostly produced from this linear isomer. The opposite should hold for the H_2 loss: in this case, removing H_2 from CH_3CN^+ is energetically less expensive than removing it from L1, so that H_2 should mostly be produced from CH_3CN^+. As the passage from CH_3CN^+ to L1 requires additional time, it is thus reasonable to expect that H emission will take longer than H_2 emission. This is precisely what can be seen in Figure 3: the H_2^+ yield saturates earlier than the H^+ yield (see also Table 1). Furthermore, the fact that H_2 ejection is a direct process and H ejection goes through the intermediate state L1 (see Figure 4) implies that the saturation time of the H_2^+ yield should be similar to that of the NHM yield, and the saturation time of the H^+ yield should be similar to those of the SHM and DHM yields. This is indeed what Figure 3 shows, the H_2^+ and NHM curves nearly overlap (except at very short times) and the H and DHM curves have similar slopes and saturate much later. This experimental finding reinforces our argument about the crucial role of the L1 isomer in the fragmentation dynamics of the acetonitrile cation.

The conclusions obtained from the above, purely stationary picture are reinforced by the fact that most vibrational modes involving C−H stretching are significantly weakened when an electron is removed from the neutral molecule (see the Supporting Information for further details), thus favoring the H-migration channels with respect to those involving C−C or C−N bond breakup.

In summary, we have used IR pump−IR probe spectroscopy in combination with ion coincident Coulomb explosion imaging to study H-migration processes in the acetonitrile cation. Our measurements allowed us to observe both single and double hydrogen migration and to discover a surprising feature: isomerization is significantly more likely than direct C−C breakup leading to fragmentation of the cation. This in spite of the fact that isomerization requires both bond breaking and bond formation. State-of-the-art theoretical modeling allows us to characterize this effect to be due to sequential isomerization processes in subsequent potential wells providing longer shifts in the fragmentation. The active role of these intermediate isomers is also apparent in the H^+ emission channel. Furthermore, we have extracted the time scales of the different processes by varying the pump−probe delay with femtosecond resolution. The experimentally measured time constants are supported by the theoretical findings. A direct characterization of some of the isomers predicted theoretically, e.g., the L2 form in which the positions of the N and C atoms are interchanged, call for future experiments in which higher order coincidences as well as Newton and Dalitz plots are analyzed. Our combined theoretical and experimental investigation demonstrates a proof-of-concept to study complex fragmentation mechanisms in detail, in particular, to identify significant molecular reorganization in ionized molecules and characterize the time needed for such isomerization processes.

METHODS

The experimental setup has been previously described elsewhere.[5] We used a 10 kHz Ti:sapphire laser producing 35 fs pulses with a central wavelength of 800 nm. The laser beam was split (50:50) into two arms time-delayed with respect to each other, each with intensities of 3×10^{14} W/cm^2. Afterward, the beams were propagated into the spectrometer where they were overlapped and back focused to a spot size of

https://dx.doi.org/10.1021/acs.jpclett.0c01344
J. Phys. Chem. Lett. 2020, 11, 6724−6729

about 10 μm with a time resolution of about 50 fs. Both beams were linearly polarized in the time-of-flight axis of the spectrometer. A molecular jet of acetonitrile, from a room temperature bubbler, was produced by expansion through a 30 μm nozzle and propagated into the spectrometer perpendicular to the two laser pulses. Acetonitrile was ionized and resulting charged fragments were detected by a Cold Target Recoil Ion Momentum Spectrometer (COLTRIMS).[11] Using a weak, homogeneous electric field, the ions were directed toward a position-sensitive detector, which is capable of measuring the three-dimensional momentum distributions of the charged particles. For CEI, we primarily focus on measuring the fragmented ions, and for the current experimental conditions, we have an ion momentum resolution of 0.1 au. By applying the coincidence technique, we can isolate specific mass channels of acetonitrile and gain the most relevant information about the fragmentation dynamics.

Quantum chemistry calculations were carried out using the density functional theory (DFT), in particular, the B3LYP functional[13,14] in combination with the 6-31++G(d,p) basis set. This method was employed both in the exploration of the potential energy surface (PES) and in the ab initio molecular dynamics calculations (AIMD) simulations. In the PES exploration, critical points in the relevant pathways were located (minima and transition states that connect them). AIMD simulations were carried out using the Atom-centered Density Matrix Propagation method (ADMP).[15−18] All the simulations have been carried out with the Gaussian16 program.[19] Further computational details are given in the Supporting Information. The combination of AIMD with PES exploration was used with success in the past to study the fragmentation dynamics of ionized molecules of different natures.[5,20−25]

■ ASSOCIATED CONTENT

Supporting Information

The Supporting Information is available free of charge at https://pubs.acs.org/doi/10.1021/acs.jpclett.0c01344.

Experimental and theoretical information of Coulomb explosion imaging, theoretical analysis, molecular dynamics, H^+/H_2^+ dissociation, global fitting, and data extraction (PDF)

■ AUTHOR INFORMATION

Corresponding Authors

Matteo McDonnell − *Department of Physics, University of Connecticut, Storrs, Connecticut 06269, United States*; Email: matteo.mcdonnell@uconn.edu

Aaron C. LaForge − *Department of Physics, University of Connecticut, Storrs, Connecticut 06269, United States*; orcid.org/0000-0002-5758-6917; Email: aaron.laforge@uconn.edu

Sergio Díaz-Tendero − *Departamento de Química, Módulo 13, Condensed Matter Physics Center (IFIMAC), and Institute for Advanced Research in Chemical Sciences(IAdChem), Universidad Autónoma de Madrid, 28049 Madrid, Spain*; orcid.org/0000-0001-6253-6343; Email: sergio.diaztendero@uam.es

Fernando Martín − *Departamento de Química, Módulo 13 and Condensed Matter Physics Center (IFIMAC), Universidad Autónoma de Madrid, 28049 Madrid, Spain; Instituto Madrileño de Estudios Avanzados en Nanociencia (IMDEA-Nano), Campus de Cantoblanco, 28049 Madrid, Spain; Donostia International Physics Center (DIPC), 20018 Donostia-San Sebastián, Spain*; orcid.org/0000-0002-7529-925X; Email: fernando.martin@uam.es

Nora Berrah − *Department of Physics, University of Connecticut, Storrs, Connecticut 06269, United States*; Email: nora.berrah@uconn.edu

Authors

Juan Reino-González − *Departamento de Química, Módulo 13, Universidad Autónoma de Madrid, 28049 Madrid, Spain*

Martin Disla − *Department of Physics, University of Connecticut, Storrs, Connecticut 06269, United States*

Nora G. Kling − *Department of Physics, University of Connecticut, Storrs, Connecticut 06269, United States*

Debadarshini Mishra − *Department of Physics, University of Connecticut, Storrs, Connecticut 06269, United States*

Razib Obaid − *Department of Physics, University of Connecticut, Storrs, Connecticut 06269, United States*

Margaret Sundberg − *Department of Physics, University of Connecticut, Storrs, Connecticut 06269, United States*

Vít Svoboda − *Laboratory of Physical Chemistry, ETH Zürich, 8093 Zürich, Switzerland*

Complete contact information is available at: https://pubs.acs.org/10.1021/acs.jpclett.0c01344

Notes

The authors declare no competing financial interest.

■ ACKNOWLEDGMENTS

The experimental work was funded by the National Science Foundation (NSF) under Award No. 1700551. Matteo McDonnell thanks the NSF REU support he received via UConn Award No. 1700551. The theoretical work was funded by the MICINN - Spanish Ministry of Science and Innovation−Ministerio Español de Ciencia e Innovación for Projects FIS2016-77889-R and CTQ2016-76061-P, "Severo Ochoa" Programme for Centres of Excellence in R & D (Grant SEV-2016-0686), and "María de Maeztu" Programme for Units of Excellence in R & D (Grant CEX2018-000805-M). We acknowledge the generous allocation of computer time at the Centro de Computación Científica at the Universidad Autónoma de Madrid (CCC-UAM).

■ REFERENCES

(1) Levine, B. G.; Martínez, T. J. Isomerization through conical intersections. *Annu. Rev. Phys. Chem.* **2007**, *58*, 613−634.

(2) Suits, A. G. Roaming Reactions and Dynamics in the van der Waals Region. *Annu. Rev. Phys. Chem.* **2020**, *71*, 77.

(3) Hishikawa, A.; Matsuda, A.; Fushitani, M.; Takahashi, E. J. Visualizing recurrently migrating hydrogen in acetylene dication by intense ultrashort laser pulses. *Phys. Rev. Lett.* **2007**, *99*, 258302.

(4) Zhao, J.; Song, T.; Xu, M.; Quan, Q.; Siu, K. M.; Hopkinson, A. C.; Chu, I. K. Intramolecular hydrogen atom migration along the backbone of cationic and neutral radical tripeptides and subsequent radical-induced dissociations. *Phys. Chem. Chem. Phys.* **2012**, *14*, 8723−8731.

(5) Kling, N. G.; Diaz-Tendero, S.; Obaid, R.; Disla, M. R.; Xiong, H.; Sundberg, M.; Khosravi, S. D.; Davino, M.; Drach, P.; Carroll, A. M.; Osipov, T.; Martin, F.; Berrah, N.; et al. Time-resolved molecular dynamics of single and double hydrogen migration in ethanol. *Nat. Commun.* **2019**, *10*, 2813.

(6) Vager, Z.; Naaman, R.; Kanter, E. Coulomb explosion imaging of small molecules. *Science* **1989**, *244*, 426−431.

(7) Stapelfeldt, H.; Constant, E.; Sakai, H.; Corkum, P. B. Time-resolved Coulomb explosion imaging: A method to measure structure and dynamics of molecular nuclear wave packets. *Phys. Rev. A: At., Mol., Opt. Phys.* **1998**, *58*, 426.
(8) Gagnon, J.; Lee, K. F.; Rayner, D.; Corkum, P.; Bhardwaj, V. Coincidence imaging of polyatomic molecules via laser-induced Coulomb explosion. *J. Phys. B: At., Mol. Opt. Phys.* **2008**, *41*, 215104.
(9) Corrales, M.; González-Vázquez, J.; de Nalda, R.; Bañares, L. Coulomb explosion imaging for the visualization of a conical intersection. *J. Phys. Chem. Lett.* **2019**, *10*, 138−143.
(10) Burger, C.; Atia-Tul-Noor, A.; Schnappinger, T.; Xu, H.; Rosenberger, P.; Haram, N.; Beaulieu, S.; Legare, F.; Alnaser, A.; Moshammer, R.; et al. Time-resolved nuclear dynamics in bound and dissociating acetylene. *Struct. Dyn.* **2018**, *5*, 044302.
(11) Ullrich, J.; Moshammer, R.; Dörner, R.; Jagutzki, O.; Mergel, V.; Schmidt-Böcking, H.; Spielberger, L. Recoil-ion momentum spectroscopy. *J. Phys. B: At., Mol. Opt. Phys.* **1997**, *30*, 2917.
(12) Eland, J. Dynamics of fragmentation reactions from peak shapes in multiparticle coincidence experiments. *Laser Chem.* **1991**, *11*, 259−263.
(13) Becke, A. D. Density-functional thermochemistry. III. The role of exact exchange. *J. Chem. Phys.* **1993**, *98*, 5648−5652.
(14) Lee, C.; Yang, W.; Parr, R. G. Development of the Colle-Salvetti correlation-energy formula into a functional of the electron density. *Phys. Rev. B: Condens. Matter Mater. Phys.* **1988**, *37*, 785−789.
(15) Schlegel, H. B.; Millam, J. M.; Iyengar, S. S.; Voth, G. A.; Daniels, A. D.; Scuseria, G. E.; Frisch, M. J. Ab initio molecular dynamics: Propagating the density matrix with Gaussian orbitals. *J. Chem. Phys.* **2001**, *114*, 9758−9763.
(16) Iyengar, S. S.; Schlegel, H. B.; Millam, J. M.; Voth, G. A.; Scuseria, G. E.; Frisch, M. J. Ab initio molecular dynamics: Propagating the density matrix with Gaussian orbitals. II. Generalizations based on mass-weighting, idempotency, energy conservation and choice of initial conditions. *J. Chem. Phys.* **2001**, *115*, 10291−10302.
(17) Schlegel, H. B.; Iyengar, S. S.; Li, X.; Millam, J. M.; Voth, G. A.; Scuseria, G. E.; Frisch, M. J. Ab initio molecular dynamics: Propagating the density matrix with Gaussian orbitals. III. Comparison with Born−Oppenheimer dynamics. *J. Chem. Phys.* **2002**, *117*, 8694−8704.
(18) Iyengar, S. S.; Schlegel, H. B.; Voth, G. A. Atom-Centered Density Matrix Propagation (ADMP): Generalizations Using Bohmian Mechanics. *J. Phys. Chem. A* **2003**, *107*, 7269−7277.
(19) Frisch, M. J. et al. *Gaussian16*, rev. C.01; Gaussian Inc: Wallingford, CT, 2016.
(20) Capron, M.; Díaz-Tendero, S.; Maclot, S.; Domaracka, A.; Lattouf, E.; Lawicki, A.; Maisonny, R.; Chesnel, J.-Y.; Méry, A.; Poully, J.-C.; et al. A Multicoincidence Study of Fragmentation Dynamics in Collision of γ-Aminobutyric Acid with Low-Energy Ions. *Chem. - Eur. J.* **2012**, *18*, 9321−9332.
(21) Maclot, S.; Piekarski, D. G.; Domaracka, A.; Mery, A.; Vizcaino, V.; Adoui, L.; Martín, F.; Alcamí, M.; Huber, B. A.; Rousseau, P.; et al. Dynamics of glycine dications in the gas phase: ultrafast intramolecular hydrogen migration versus Coulomb repulsion. *J. Phys. Chem. Lett.* **2013**, *4*, 3903−3909.
(22) Piekarski, D. G.; Delaunay, R.; Maclot, S.; Adoui, L.; Martín, F.; Alcamí, M.; Huber, B. A.; Rousseau, P.; Domaracka, A.; Díaz-Tendero, S. Unusual hydroxyl migration in the fragmentation of β-alanine dication in the gas phase. *Phys. Chem. Chem. Phys.* **2015**, *17*, 16767−16778.
(23) Kukk, E.; Ha, D.; Wang, Y.; Piekarski, D. G.; Díaz-Tendero, S.; Kooser, K.; Itälä, E.; Levola, H.; Alcamí, M.; Rachlew, E.; Martín, F. Internal energy dependence in X-ray-induced molecular fragmentation: an experimental and theoretical study of thiophene. *Phys. Rev. A: At., Mol., Opt. Phys.* **2015**, *91*, 043417.
(24) Maclot, S.; Delaunay, R.; Piekarski, D. G.; Domaracka, A.; Huber, B.; Adoui, L.; Martín, F.; Alcamí, M.; Avaldi, L.; Bolognesi, P.; et al. Determination of energy-transfer distributions in ionizing ion−molecule collisions. *Phys. Rev. Lett.* **2016**, *117*, 073201.
(25) Piekarski, D. G.; Delaunay, R.; Mika, A.; Maclot, S.; Adoui, L.; Martín, F.; Alcamí, M.; Huber, B. A.; Rousseau, P.; Díaz-Tendero, S.; et al. Production of doubly-charged highly reactive species from the long-chain amino acid GABA initiated by Ar^{9+} ionization. *Phys. Chem. Chem. Phys.* **2017**, *19*, 19609−19618.

https://dx.doi.org/10.1021/acs.jpclett.0c01344
J. Phys. Chem. Lett. 2020, 11, 6724−6729